Mass Transfer and Solubility in Autocatalytic Oxidation of Cyclohexane

Mass transfer coefficients for the solution, without reaction, of oxygen in cyclohexane over a wide range of temperature and pressure have been measured in a flat interface reactor (FIR) and a gas sparged stirred-tank reactor (STR). Solubilities have also been measured and it is suggested that a modified Henry's law coefficient of 1.09×10^{-2} kmol/m^3 · bar can be regarded as constant over the temperature range 293-435 K. The physical mass transfer coefficient in the STR shows very little variation over this temperature range and a value of 3.5×10^{-4} m/s can be assumed for 423-435 K. However, coefficients in the FIR increase with agitation rate as expected. The difference is ascribed to interference by neighboring bubbles in the transfer process, when diffusivities are high, and also to the lowering of surface tension at high temperatures. A model proposed by Gal-Or and Resnick is reviewed in its application to the present system.

A. K. Suresh, T. Sridhar, O. E. Potter
Department of Chemical Engineering
Monash University
Clayton, Victoria 3168, Australia

Introduction

A knowledge of the solubility and mass transfer coefficients of oxygen in cyclohexane at the temperatures of oxidation is necessary to separate the effect of mass transfer from that of reaction kinetics in the observed absorption rates in the gas-liquid mode of contacting. The mass transfer coefficient is also a quantity of fundamental importance, since its magnitude and the nature of its dependence on the physicochemical and turbulence parameters can shed light on mass transfer behavior.

This paper describes the measurement of mass transfer coefficients for oxygen in cyclohexane over a range of temperatures in two types of gas-liquid contactors: a flat interface contactor that features mass transfer across the free interface of a well-stirred liquid, and a sparged and agitated vessel in which mass transfer is from bubble swarms to a well-stirred liquid.

Even though several theories of mass transfer at an interface have been proposed, most such theories have a parameter that depends on the turbulent flow field, and hydrodynamics in the mechanically stirred vessel are still not well understood so that predictions are at least partly based on empiricism. The experimentally measured quantity is usually the volumetric mass transfer coefficient. For a flat interface contactor, the mass transfer area is fixed and therefore variations in k_La reflect those in the true mass transfer coefficient. While this is not true with bubbling contactors (the interfacial area for mass transfer being a complicated function of the geometry, power input, sparging, and the physical properties of the liquid), over fairly wide ranges of operating variables for a given system, the mass transfer coefficient can be considered a constant (Sideman et al., 1966). For this reason and also because of the difficulties in measuring interfacial areas under given hydrodynamic conditions, it is most often the volumetric mass transfer coefficient that is correlated, although it would be advantageous to study the effect of the various operating variables on k_L and a separately.

A theory that attempts to describe the process of mass transfer to or from a turbulent system must take into account the two mechanisms responsible: molecular diffusion and turbulent mixing. Several such theories have been proposed in the literature and the more important ones have been discussed at length in several textbooks (Astarita, 1967; Danckwerts, 1970; Sherwood et al., 1975). The film and penetration type approaches consider mass transfer close to the interface to take place by a molecular mechanism. The film theory considers a steady state process through a stagnant film, while the penetration (and surface renewal) theories consider an unsteady state mass transfer into fluid elements that behave as rigid bodies during their stay at the interface.

The specific case of transfer from bubbles or drops has been considered in some detail. The convective diffusion equation for a sphere in free rise or fall is taken as the starting point, and several such analyses have been reviewed (Ruckenstein, 1964;

A.K. Suresh is currently with Hindusthan Lever Research Center, Bombay, India.

Calderbank, 1967; Resnick and Gal-Or, 1968). The steady state situation is the one most extensively studied, but even here the complexity of the problem permits analytical solutions to be obtained only in certain asymptotic cases. Aspects of mass transfer in bubble swarms have been discussed by Calderbank and Moo-Young (1961), Hughmark (1967), and Schaftlein and Russell (1986).

Experimental Techniques

The methods used to measure mass transfer coefficients in gas-liquid contactors generally yield the volumetric mass transfer coefficient k_La. These methods can be broadly classified into physical and chemical methods, depending on the type of absorption used in the experiment. These methods have been recently reviewed by van't Riet (1979) and Mann (1983).

Physical methods

The most popular dynamic physical absorption-desorption method consists in following the response of the liquid phase to a step change in the gas phase concentration. The method requires the sampling of the liquid phase at frequent intervals. The advent of fast dissolved oxygen probes in the last fifteen years has led to extensive use of this method with the oxygen-water system under ambient conditions.

Mathematical methods of varying complexity have been used to describe the transients in these experiments (Calderbank, 1959; Dunn and Einsele, 1975; Dang et al., 1977; Linek et al., 1981; Ruchti et al., 1981), and the usefulness of the various models in the face of the errors that result from the simplifications involved has been reviewed (Ruchti et al., 1981; Linek et al., 1982).

Although the methods described above are of general applicability, they have mostly been used with the oxygen-water system under ambient conditions, first because of the importance of such studies to biochemical processes, but more importantly because of the availability of the oxygen probe to measure rapid transients.

Chemical methods

In the chemical methods, a reaction of known kinetics is made to occur in a desired regime of absorption by choosing a suitable concentration of the liquid phase reactant or otherwise adjusting the reaction rate. From the measured absorption rate, the mass transfer parameter of interest is obtained with the aid of a suitable theory of mass transfer with chemical reaction. Since the absorption rate depends on different factors in different regimes, different mass transfer parameters can be evaluated depending on the regime. Sharma and Danckwerts (1970) give a detailed account of the possibilities; Mann (1983) adds further information. An exhaustive list of the reactions used in interfacial area measurements by the chemical method is contained in the recent review by Midoux and Charpentier (1984). Ruchti et al. (1985) note that the combined effect of the chemical enhancement and the increase in interfacial area due to the presence of ionics can be to increase the measured volumetric mass transfer coefficient more than tenfold compared with physical measurements in air-water systems.

A further difficulty with the application of the chemical methods to a complex hydrodynamic situation such as exists in the STR is that different regimes might be operating in different parts of the same contactor. It is known (Cutter, 1966) that the rate of energy dissipated varies quite dramatically across a cross section of the vessel. Such variations are likely to result in local variations in the mass transfer coefficient and hence, the Hatta number. Sridhar and Potter (1978) found that the sulfite method consistently overestimated the interfacial area as compared to the light-scattering method, a fact which they found could be explained by such local variations.

Equipment Description

A schematic flow diagram of the stirred-tank reactor (STR) system is shown in Figure 1. High-purity nitrogen, metered, heated nearly to the reactor temperature, and saturated with cyclohexane vapors at the reactor temperature is mixed with high-purity oxygen, also metered, at the base of the reactor. The reactor has a specially designed sparger to aid thorough mixing of the gases. The mixed gases are sparged into the reactor where they undergo a process of absorption and reaction. The gases leaving the reactor pass through a series of three condensers where cold water is used to condense out cyclohexane vapors as well as any water formed during the reaction. The uncondensed gases pass through a back-pressure regulator into the exhaust. The condensed liquid drains through a packed bed of Raschig rings where any dissolved oxygen is stripped by a countercurrent stream of high-purity nitrogen. The condensate collects in a separator where any water along with dissolved products settles to the bottom. The hydrocarbon layer is pumped back into the saturator. Further details may be found in Suresh (1986).

All the vessels containing hot cyclohexane are housed in an enclosure made of 0.5 cm thick steel panels. The enclosure is filled with CO_2 gas and is maintained at the temperature of the reactor. Glass windows provided in front of the reactor windows enabled visual inspection of the reactor contents. Temperature control in the reactor is effected by circulating the liquid contents continuously through an external heat exchanger.

The reactor is a 0.13 m dia. stirred tank, flanged at both ends, of conventional geometry (Rushton et al., 1950). Except for the position and dimensions of some inlets and outlets, the vessel is identical to that described previously by Sridhar and Potter (1980b).

A schematic diagram of the flat interface reactor (FIR) is shown in Figure 2. The gas-liquid contact area in this reactor is about 30–40 times smaller than in the stirred-tank reactor. Hence, the absorption rates in this reactor can be anticipated to be correspondingly smaller. The gas is introduced into the reactor above the liquid, and transfer takes place across the free surface of the liquid as the gas passes over it. The gases from the reactor pass through a back-pressure regulator that maintains the pressure in the reactor, and bubble through a pool of cold water in a closed vessel, losing much of the cyclohexane vapors in the process. The gases leave the equipment through a vent line.

The reactor normally operates at a pressure of 13–14 bar. It is identical in internal geometry to the sparged reactor except for the spatial arrangement of some inlets and outlets. Both the gas and the liquid phases are stirred in this reactor by turbine stirrers supported on a common shaft and rotated by a magnetic drive. The stirrer in the liquid is identical to that used in the STR described earlier. The stirrer in the gas phase is of larger dimensions (0.068 m dia., 0.012 m blade width). Product samples as well as liquid samples for dissolved oxygen analysis are

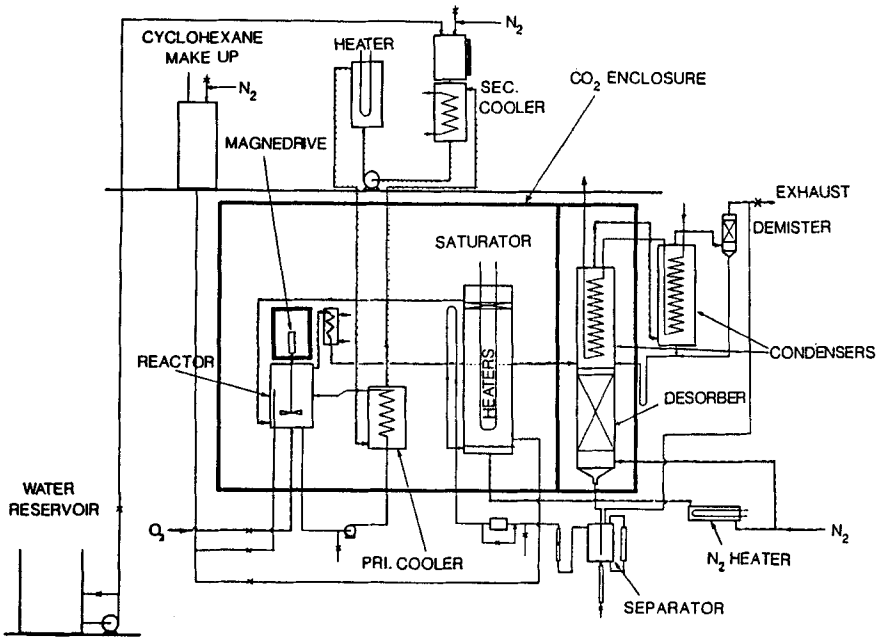

Figure 1. Flow diagram of stirred-tank reactor (STR) equipment.

taken from a centrally located hole in the base of the reactor through a needle valve.

The reactor is housed in a heated chamber filled with carbon dioxide. Bayonet heaters of 5 kW capacity are fitted to the front cover of the chamber and serve to heat the carbon dioxide; a circulator helps to keep the temperature uniform within the box. The reactor itself is heated or cooled from the outside by the carbon dioxide. Two stainless steel sheathed thermocouples, one in the liquid and the other in the gas, monitor the temperature in the reactor. Temperature control is effected by a Eurotherm controller that controls the power supply to the bayonet heaters depending on the temperature in the liquid. The pressure in the reactor is measured by a 0–300 psi (0–2 MPa) Budenberg pressure gauge.

The oxygen absorption rate is calculated from the difference between the concentrations of oxygen in the reactor inlet and outlet gases. The oxygen content of the reactor outlet gases is determined using a polarographic oxygen electrode. For this purpose, a continuous bleed of the gases leaving the reactor is drawn as a sample.

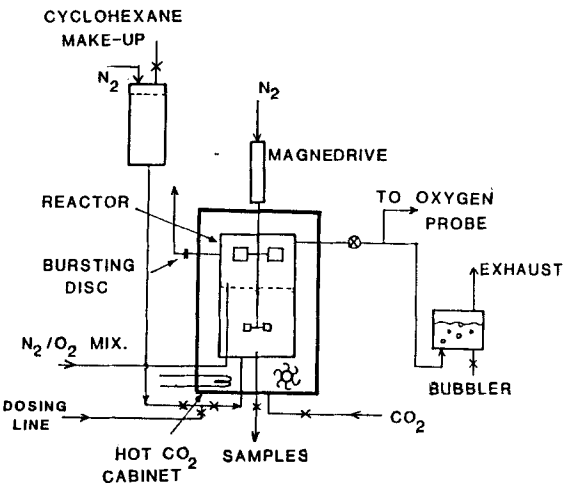

Figure 2. Diagram of flat interface reactor (FIR) equipment.

Samples of the oxidate are taken frequently and stored at temperatures of about 253 K for later analysis. Samples for dissolved oxygen analysis are analyzed immediately after they are taken. Both samples are taken from the circulating liquid in the heat transfer loop, at the inlet to the circulating micropump. Care has been taken in the design of this circuit so that no gas bubbles are present in the liquid and so that the residence time of the liquid in the lines before the sampling point is sufficiently small for reaction in the lines to be neglected.

The product samples are first let into a coiled tube by opening and closing a ball valve. After the sample has cooled sufficiently (cold water can be used to cool the coil), it is removed into a vial by opening a needle valve and a bleed valve (to bleed in air). The sample volume of about 7 mL is quite small in comparison to the batch volume, and taking samples does not interfere with the course of the reaction.

The gases are desorbed from solution by a pressure letdown and analyzed for oxygen content using a gas chromatograph. This can then be translated into the oxygen content in the liquid.

By opening a needle valve, a volume of the reactor liquid from the circulating stream is passed through a piece of 3 mm Teflon tubing into a vial filled with water and held inverted in a tank of water. Most of the dissolved gases (oxygen and nitrogen) desorb and collect on top of the hydrocarbon, which itself collects on top of the water. This gas is then drawn into the sampling loop of the Carle sampling valve by applying a slight suction with a syringe. Switching the valve injects this gas sample into the carrier gas stream, which passes through a precolumn of 3 mm ID and 1.3 m length, packed with silica gel to retain any residual cyclohexane vapors. The sample then passes through another column in

the chromatograph oven packed with molecular sieve 5A. Although this column is not essential for the analysis, it can be used to get an absolute calibration of the detector by injecting different volumes of air into the injection port of the chromatograph and was retained for this purpose. The sample then passes into the detector of the chromatograph. An electron capture detector was used. This detector is highly sensitive and is specific to compounds exhibiting an electron affinity. In a mixture of oxygen and nitrogen, therefore, only oxygen evokes a response from the detector. The response of the detector is recorded and integrated by a Hewlett-Packard integrator.

Solubility measurements

When mass transfer is accompanied by chemical reaction, the dissolved gas concentration will, in general, be lower than the saturation value. Solubilities under such conditions are therefore measured, as a rule, indirectly, by measuring the absorption rate in a situation that can be hydrodynamically well described or by interpreting the measured absorption rates using a theory of mass transfer with chemical reaction (Danckwerts, 1970). In the present case, however, the existence of the induction period for the reaction has been exploited to measure solubilities directly from the dissolved oxygen levels during the initial part of the reaction experiments. The induction period in a free radical reaction is the time taken for a sizable concentration of free radicals to build up so that the chain reaction can sustain itself. This period is characterized by a negligible reaction rate. When an oxygen-nitrogen mixture is first brought into contact with cyclohexane maintained at the temperature and pressure necessary for reaction, the liquid soon becomes saturated with oxygen at the prevailing partial pressure and remains saturated for a time before the reaction rate becomes fast enough to consume oxygen at a rate higher than that at which it is supplied by mass transfer. Solubilities can therefore be measured by measuring dissolved oxygen levels during such an induction period.

Solubility measurements at the lower temperatures were mainly performed in the FIR. Analytical grade cyclohexane was used in all experiments. The liquid in the reactor was brought up to the required temperature under nitrogen pressure and allowed to become saturated with nitrogen at the operating temperature and pressure. The flow of an oxygen-nitrogen mixture into the reactor was then begun. Dissolved oxygen concentrations were measured by taking samples and analyzing them in the gas chromatograph as described earlier. For solubility measurement, samples were taken well beyond the time when the dissolved oxygen levels ceased to vary.

The final concentrations measured correspond to saturation at the prevailing partial pressure of oxygen. Under these conditions, the oxygen level at the exit would be the same as at the inlet on a cyclohexane vapor-free basis, but a knowledge of the partial pressure of cyclohexane is necessary to evaluate the partial pressure of oxygen. The partial pressure of cyclohexane in the exit gases was determined as follows. With the liquid saturated with nitrogen, dissolved nitrogen was desorbed from the liquid by letting a sample of the liquid down to atmospheric pressure. The desorbed gas is almost entirely nitrogen and its volume can be related to the nitrogen dissolved in the reactor, from which, in turn, the partial pressure of nitrogen in the reactor can be calculated, using the Henry's law coefficient for nitrogen reported by Wild et al. (1978). The difference of this from the total pressure then gives the partial pressure of cyclohexane, which can be compared with the published data on the vapor pressure of cyclohexane (Gallant, 1970; Yaws and Turnbough, 1975). The gases were found to be saturated with cyclohexane vapor in all the experiments.

Mass transfer coefficients

Volumetric mass transfer coefficients were measured in the FIR and the STR over a range of temperatures spanning the ambient temperature and the reaction temperatures. A single method was not suitable over this entire range; accordingly, three methods were employed and the relevant theoretical and experimental details follow. The determination of the mass transfer coefficient at the reaction temperatures was given special attention, being made over several runs, where possible using more than one method.

The dynamic physical method was used in both types of contactors. In the case of the STR, a feature of the reaction under study—the induction' period—was exploited to enable the use of the physical method right up to 423 K, where the possibility of reaction would normally make the use of this method impossible. Due to the small values of the volumetric mass transfer coefficient (long times required for saturation of the liquid) and the short duration of the induction period, the use of the physical method in the FIR had to be restricted to temperatures of less than 403 K.

In the Appendix, the coupled material balances for a solute that is transferred from a gas phase into a liquid phase (or vice versa) is set up and solved for the case of unequal gas flow rates at the inlet and outlet of the contactor.

The volumetric mass transfer coefficient can be found by fitting the experimental response to Eq. A10 by a nonlinear regression procedure. Under some circumstances, however, the last term in Eq. A10 can be neglected and some simplification results, so that parameter estimation can be performed using a semilogarithmic plot of $(1 - c_l)$ vs. time.

Procedure

Analytical grade cyclohexane (Malinckrodt) was used in all the experiments. An initial steady state was established by saturating the liquid at the operating temperature and pressure (usually about 12–13 bar) with nitrogen saturated with cyclohexane, the liquid being kept stirred at the required speed. In the case of the FIR, the step change was made to 4% oxygen at the gas manifold upstream of a bank of rotameters, maintaining constant flow. The time delay, between the point at which the step change was made and the reactor, was confirmed to be negligible, and the Reynolds numbers for flow in these lines were sufficiently high for plug flow to be assumed. This and other lags such as sampling were lumped together as a dead time in the analysis of experimental data. Samples for dissolved oxygen analysis were withdrawn at intervals and analyzed. The oxygen content of the gases leaving the contactor was continuously monitored. An absorption run was usually followed by a desorption run. 4% oxygen in nitrogen (premixed, Commonwealth Industrial Gases) was used in most experiments, but for purposes of comparison a few runs at near-ambient temperatures were carried out using high-purity oxygen. The entering gases were free from cyclohexane vapors, and it was confirmed that the leaving gases were saturated with cyclohexane.

In the case of the STR, the nitrogen was presaturated with

cyclohexane in the saturator and mixed with a small percentage (usually 4%) of oxygen at the base of the reactor. Step changes for absorption and desorption were made by respectively opening and closing the oxygen solenoid valve near the reactor. Gas superficial velocity was not altered significantly by such addition or stoppage of the oxygen stream.

To compare the present technique with the use of the conventional dissolved oxygen electrode, one experiment at 303 K was carried out at atmospheric pressure, using the probe as well as the gas chromatographic methods of analysis for dissolved oxygen. Since the probe could not be housed within the reactor, a pump was used to circulate the liquid at a high rate through an external loop in which the probe was housed. For analysis by gas chromatography, liquid samples were taken from a location close to the oxygen probe as well as from the usual sampling point at the bottom of the reactor and were injected using the Carle sampling valve.

Chemical method

Volumetric mass transfer coefficients at 433 K were obtained in the FIR from measurements of the oxygen absorption rate in the diffusional regime. The oxidation of cyclohexane exhibits autocatalysis with the absorption rates increasing as reaction products increase. Hence, in principle, a reaction that starts off in the kinetic regime can be expected to run into the diffusional regime when the reaction was accelerated sufficiently. The onset of the diffusional regime can be determined by following the decline of the dissolved oxygen concentration in the liquid with time. This procedure was followed in the FIR. After oxygen was admitted into the reactor maintained at temperature and pressure, the liquid was sampled at intervals for oxygen. The oxygen concentration was observed to rise, to start decreasing almost immediately, and ultimately to reach zero after about 9–12 min. The absorption rate remained constant after this time. The procedure utilizing the dissolved oxygen analysis therefore circumvented the difficulties normally experienced with identification of the diffusional regime.

The rate of oxygen absorption under these circumstances is given by

$$R_A = k_L a\, c^* \tag{1}$$

c^* is related to the exit gas composition (under the assumption of well-mixed gas phase), which was determined from the measured oxygen content of the exit gas the vapor pressure of cyclohexane at the reactor temperature, the exit gases being saturated with cyclohexane vapors.

The chemical method could not be used in the STR because the dissolved oxygen showed a tendency to oscillate before dropping to zero, thus making it difficult to establish the onset of the diffusional regime, and there was no extended period of a constant absorption rate once the dissolved oxygen went to zero.

Dissolved oxygen–exit oxygen (DO-EO) plot

A new method was devised to determine the mass transfer coefficients in the STR during reaction in the slow reaction regime. Because of autocatalysis, the absorption rates increase continuously and the existence of an extended slow reaction regime with such a reaction provides the possibility of measuring the absorption rates over a range of mass transfer driving forces in a single run. It is assumed that the mass transfer is not chemically enhanced during this period. Astarita's (1967) argument that the reaction should become fast enough to deplete the liquid of oxygen before it can become fast enough to chemically enhance the mass transfer supports this assumption.

The present method also makes the assumptions of pseudo-steady state in the gas phase and a well-mixed gas phase in the dispersion. The variation of absorption rate is sufficiently small and the gas phase transients sufficiently fast to justify the former, while the usually small extent of depletion of oxygen in the gas phase makes any errors resulting from the latter assumption quite small. A material balance for oxygen in the gas phase yields, under these assumptions,

$$q_i - q_o = k_L a V_{GL} (c^* - c_1) \tag{2}$$

where q_i and q_o are respectively the flow-rates of oxygen into and out of the reactor. c is related to the exit oxygen partial pressure and hence q_o by

$$c^* = H_O P (q_o / q_T) \tag{3}$$

where q_T is the total molar flow rate of the gases out of the reactor. Substitution and rearrangement gives

$$q_o = S c_1 + I \tag{4}$$

where

$$S = \frac{k_L a V_{GL}}{\left(1 + \dfrac{k_L a V_{GL} H'_O P}{q_T}\right)} \tag{5}$$

and

$$I = \frac{q_i}{\left(1 + \dfrac{k_L a V_{GL} H'_O P}{q_T}\right)} \tag{6}$$

Thus a plot of exit oxygen flow rate vs. the dissolved oxygen concentration should be linear and $k_L a$ should be calculable from the slope as well as from the intercept provided the Henry's law coefficient for oxygen is known at the temperature of reaction. Equations 5 and 6 show that, at large values of $k_L a$, the slope becomes insensitive to its value while the intercept depends on it and the converse happens at small values of $k_L a$. It may therefore be expected that the values of $k_L a$ derived from the intercept will be generally more accurate at large values of $k_L a$ while those from the slope will be more accurate at small values. At intermediate values both the slope and intercept must give comparable values, although the slope would generally be expected to give more accurate results since a small change in slope could result in a large change in the intercept.

Results and Discussion

Solubility

Solubility data for oxygen in cyclohexane have been reported up to a temperature of 373 K by Wild et al. (1978). These authors also extended the previous data on the solubility of

nitrogen in cyclohexane up to 443 K. In common with other sparingly soluble gases, oxygen and nitrogen were found to follow Henry's law over the entire range of temperatures studied. The Henry's law coefficients for oxygen were correlated by

$$\log H_O = 0.366 \log T - 3.8385 \quad (7)$$

and those for nitrogen, by

$$\log H_N = 1.2844 \log T - 6.2924 \quad (8)$$

It would be profitable to extend the range of the data on the solubility of oxygen in cyclohexane up to reaction temperatures. Further, solubility measurements at lower temperatures can be used to provide a check on the method of sampling and analysis employed in the present work to determine dissolved oxygen levels during reaction.

The solubilities measured in this work, converted to Henry's law coefficients are compared with the data of Wild et al. (1978) in Figure 3. The data for nitrogen from the same authors are also shown for comparison. The measured values up to 395 K show good agreement with the data of Wild et al., the deviation from Eq. 7 being less than 6% (with the exception of the value at 305 K, which deviates by about 10%). Such errors can easily be explained when one considers that any errors in the measurement of flow rate, pressure, and the reported values of the vapor pressure of cyclohexane go into the calculation of the partial pressure of oxygen. The data therefore indicate that the method employed for the measurement of the concentration of dissolved oxygen under conditions of high temperature and pressure can be used with confidence.

The dissolved oxygen concentrations measured during the induction period have been plotted as a function of the prevailing partial pressure of oxygen in Figure 4. Data for 413 and 423 K are shown. The linear relationship confirms the validity of Henry's law and justifies the inclusion of these data in the plot of Figure 3. The slopes of the lines for 413 K are very similar; in fact, all the measurements between 413 and 430 K gave values of the Henry's law coefficient that lie between 1.4×10^{-3} and

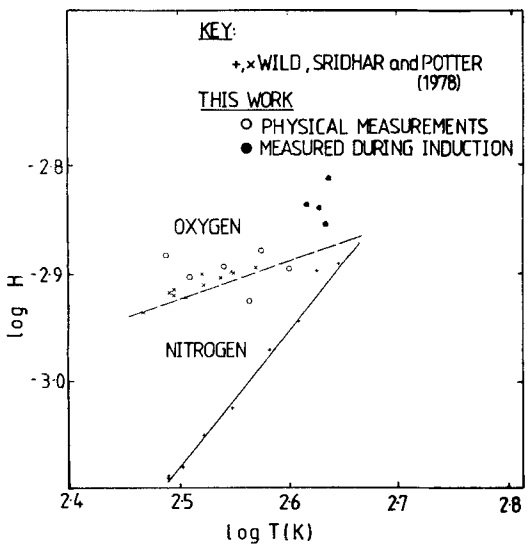

Figure 3. Variation of O_2 and N_2 solubilities in cyclohexane with temperature.

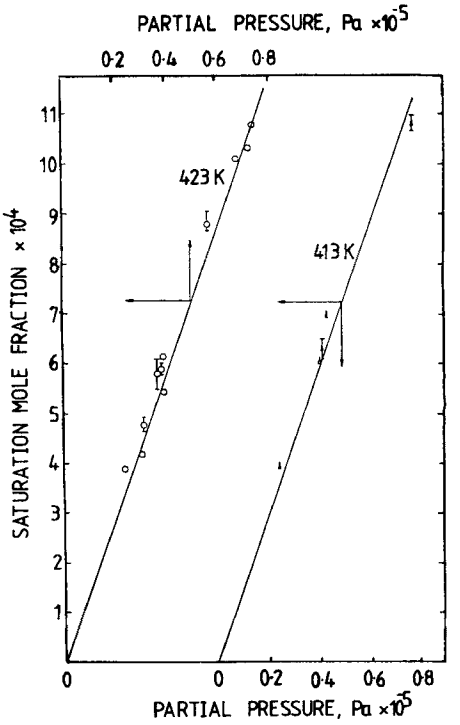

Figure 4. Plots of Henry law for O_2 in cyclohexane at 413 and 423K.

1.46×10^{-3} mol frac/bar with a limited number of measurements at 435 K averaging to a value of 1.55×10^{-3} mol frac/bar.

Referring to the comparison between the data and the data at lower temperatures in Figure 3, it is seen that Eq. 7 underestimates the value of the Henry's law coefficient at temperatures higher than 413 K by 10–15%.

Hayduk and Buckley (1971) showed, based on the data available at low temperatures, that the solubilities of all gases approach the same reference solubility as the critical temperature of the solvent is reached. However, the data of Wild et al. (1978) for temperatures above 373 K, showed upward deviations from the straight line found by Hayduk et al. (1971). This, together with similar indications found in the literature, prompted Wild et al. to suggest that linear extrapolation of the data using a reference solubility might lead to errors at higher temperatures. The present data at high temperatures of oxygen show deviations from the low-temperature data that are qualitatively similar to those found by Wild et al. for nitrogen and lend some support to this view.

The Henry's law coefficient in Figure 3 has units of mol frac/bar. While this quantity increases slightly with temperature, the density of the liquid decreases with temperature. This suggests that the solubility expressed as mol/cm^{3}bar would vary less with temperature. This quantity has been calculated from the values of H_O measured in this work as well as by Wild et al. using the values reported by Gallant (1970) for the density of cyclohexane at different temperatures and tabulated in Table 1 and shows remarkably little variation over the entire temperature range. A constant value of about 1.09×10^{-2} kmol/m^{3}bar can therefore be used for the solubility of oxygen in cyclohexane over the temperature range covered by this data.

Since the chemical composition of the liquid changes during

Table 1. Values of H_O and H'_O for Oxygen in Cyclohexane at Various Temperatures

Temp. K	$H_O \times 10^3$ mol frac/bar	$H'_O \times 10^2$ kmol/m³ · bar	Source
293	1.16	1.068	Wild et al. (1978)
309	1.21	1.093	Wild et al. (1978)
312	1.21–1.22	1.085–1.094	Wild et al. (1978)
320	1.20	1.069	Wild et al. (1978)
325	1.25	1.104	Wild et al. (1978)
332	1.231–1.26	1.082–1.107	Wild et al. (1978)
344	1.25	1.077	Wild et al. (1978)
346	1.28	1.101	This work
352–353	1.263	1.075	Wild et al. (1978)
365	1.19	1.000	This work
371	1.277	1.062	Wild et al. (1978)
375	1.33	1.098	This work
395	1.26	1.011	This work
413	1.46	1.13	This work
423	1.45	1.10	This work
430	1.40	1.053	This work
433	1.55	1.16	This work

reaction, it is important to know whether properties such as solubility are substantially affected at the conversions likely to be achieved in the reaction experiments.

Mass transfer coefficients in the FIR

At temperatures close to ambient (up to about 323 K), the values of the volumetric mass transfer coefficients were sufficiently small (less than $8 \times 10^{-4}\ s^{-1}$) for the gas phase transient to be neglected in the estimation of k_La from the experimental responses—the slope of a plot of ln $[1/(1 - c_1)]$ vs. time was in good agreement with the value of k_La estimated from the rigorous solution, eq. A10. At higher temperatures, however, the semilog plot generally gave an underestimate and the volumetric mass transfer coefficient under such circumstances was estimated by fitting the experimental response to Eq. A10 using the nonlinear regression routine ZXSSQ (IMSL Inc.).

Table 2. Comparison of Mass Transfer Coefficients Evaluated from Different Gas Exchanges

Temp. K	Gas Exchg. w/Nitrogen	Mode	$k_L \times 10^4$ m/s
293	4% oxygen	Absorption	1.04
293	Pure oxygen	Absorption	0.93
325	4% oxygen	Absorption	1.61
325	Pure oxygen	Absorption	1.43
		Desorption	1.65

The responses as measured by a conventional dissolved oxygen probe are compared in Figure 5 with the present technique employing discrete sampling and analysis by gas chromatography (GC) in the atmospheric pressure run at 303 K for the gas exchange nitrogen to oxygen. The GC data in the figure pertain to samples from two locations. The data for the desorption run (oxygen to nitrogen) for the same conditions are also shown in Figure 5. The probe response agrees well with the GC analyses, validating the present technique.

Further tests were made to ensure that the concentration of the gas used in the experiment did not influence the results. Table 2 compares the mass transfer coefficients obtained from a N_2–O_2 interchange with those from a N_2–4% O_2 interchange at two temperatures. The agreement is satisfactory.

Mass transfer coefficients were measured over a range of temperatures (293–395 K) at a stirrer speed of 150 rpm by the physical method. In these experiments, a variation in the Reynolds number occurred because of the variation in physical properties even though the stirrer speed was kept constant at 150 rpm. However, to see the effect of the stirrer speed, the mass transfer coefficients were determined by the chemical method at three stirrer speeds at 433 K. These data are shown in Figure 6. The absorption rates under these conditions are quite small and difficult to measure accurately, and the range of values determined from a number of runs is shown. A fairly linear relationship is seen to exist between the mass transfer coefficient and the stirrer speed. On a logarithmic plot, a slope slightly higher than 1 (about 1.15) is obtained, but in view of the limited number of

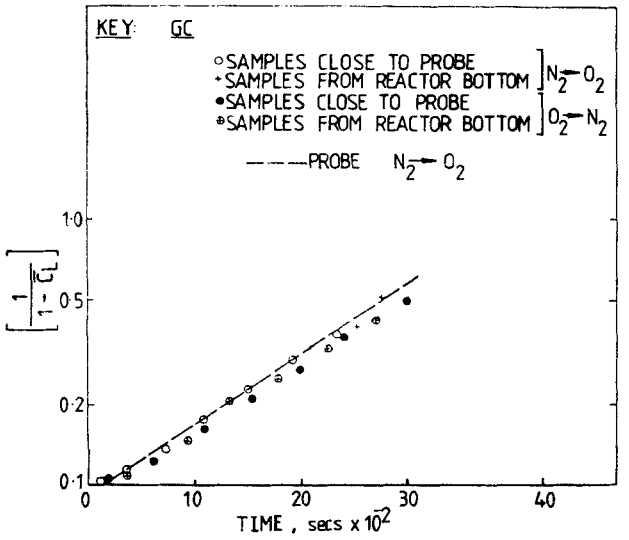

Figure 5. Comparison of continuous sampling with O_2 probe with method of discrete sampling.

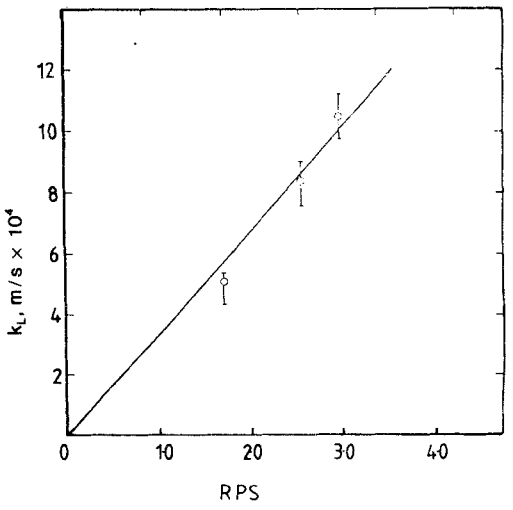

Figure 6. Effect of stirrer speed on mass transfer coefficient in FIR at 423 K.

data points and the general scatter, a value of 1 for this exponent was considered adequate.

Interpreting the observed dependence of k_L on stirrer speed as the dependence of the Sherwood number on the impeller Reynolds number in the conventional type of correlation in such contactors, the value of the ratio of the Sherwood to the Reynolds number is plotted as a function of the Schmidt number in Figure 7. In these calculations, the diffusivities were assumed to be those of nitrogen in cyclohexane (the diffusivities of oxygen and nitrogen in cyclohexane are very similar; [Lynch and Potter, 1978; Sridhar and Potter, 1978; Sridhar, 1978]), for which experimental data are available up to 413 K. Values at higher temperatures up to 436 K were obtained by extrapolating these data using

$$\frac{D\mu}{T} = \text{const.} \tag{9}$$

The values of the physical properties over the temperature range used were obtained from Gallant (1975) and Yaws and Turnbough (1975).

In spite of the scatter, a good correlation is seen in Figure 7. The equation of the regression line gives

$$Sh_T = 0.08\ Re\ Sc^{0.395} \tag{10}$$

Where the Sherwood number is based on the tank diameters, the range of the Reynolds numbers covered in these experiments was 3,900–16,000, and that of the Schmidt number 10–340. In particular, such low Schmidt numbers are rarely encountered in the vast literature on gas-liquid systems, although, as appears from the present case, quite a few industrially important processes do operate under conditions of such small Schmidt numbers.

Mass transfer coefficients in the STR

In the case of the STR, errors due to the gas phase transients were ignored. In the estimation of the volumetric mass transfer coefficient from the step response data, it is preferable to ignore the data in the initial and final 20% of the response (Sridhar, 1978). The discrete sampling method used and the short period for which the transients lasted meant that, often, not enough points were obtained in this region to produce a reliable estimate of the volumetric mass transfer coefficient from Eq. A10 by nonlinear estimation methods, although a good straight line could be fitted to the data on a semilogarithmic plot of the response. Moreover, the value estimated from the nonlinear estimation methods obtained is sensitive to the value of the gas holdup, a quantity that is usually poorly estimated, especially at low values. As will be seen later, the mass transfer coefficients so obtained agree well at the high and the low temperatures, in the former case with the values obtained from the dissolved oxygen–exit oxygen (DO-EO) plot during reaction and in the latter, with the small bubble correlation of Calderbank and Moo-Young (1961), and this indicates that the errors due to gas phase transients are small.

Calculation of the mass transfer coefficient from the experimentally measured k_La requires a knowledge of the gas-liquid interfacial area. Interfacial areas in a sparged and stirred vessel, in internal geometry identical to the reactors used in the present work, were measured by a light-transmission technique by Sridhar and Potter (1980b) for the nitrogen-cyclohexane system up to a temperature of 423 K and under a pressure of about 10 bar. Where possible, values of gas holdup and bubble diameters used in what follows are also calculated using the correlations given by Sridhar and Potter (1980a).

Volumetric mass transfer coefficients have been plotted in Figure 8 as a function of the specific power input (including the power input through the sparging and expansion of the gas, calculated as indicated by Sridhar and Potter, 1980b) at constant temperature and superficial velocity. These data can also be regarded as showing the effect of agitation rate on the volumetric mass transfer coefficient. The dependence is seen to be weak in all cases. When these data are converted to mass transfer coefficients, the values show hardly an variation at all with agitator speed, quite in agreement with the observations in other studies.

The volumetric mass transfer coefficients under the conditions of reaction, measured using the dissolved oxygen–exit oxygen plot are tabulated in Table 3. Representative plots of Eq. 4 are shown in Figure 9. The plots have a satisfactory linearity and the values of the volumetric mass transfer coefficients obtained from the slope and intercept of these plots generally

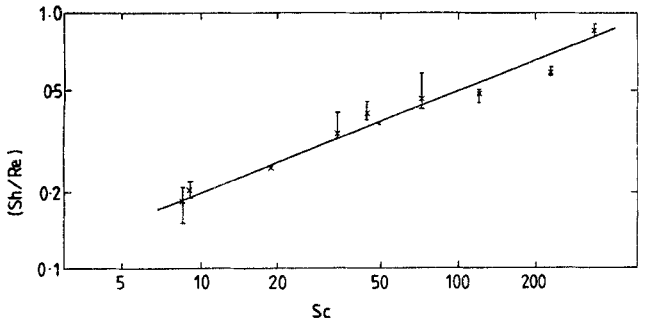

Figure 7. Correlation for mass transfer coefficients in FIR.

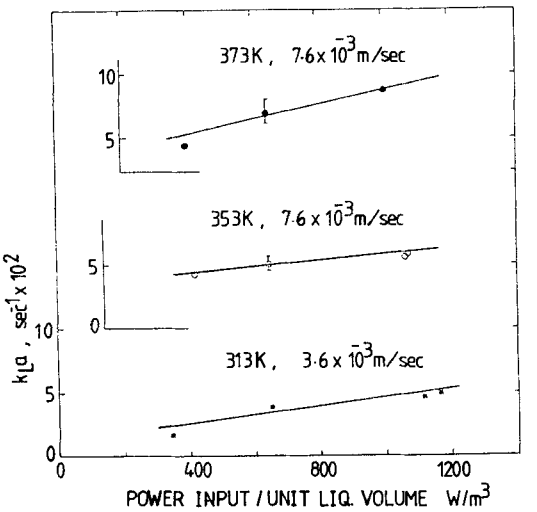

Figure 8. Variation of volumetric mass transfer coefficients with specific power input in STR, at constant temperature and superficial gas velocity.

Table 3. Volumetric Mass Transfer Coefficients During Reaction Using DO-EO Plot

Temp. K	Superfic. Veloc. m/s × 10^2	RPM	% O_2 in	k_La s^{-1}	a m^{-1}	$k_L \times 10^4$ m/s
413	0.92	1,000	1.96	0.174	414	4.2
414.5	0.98	1,000	3.6	0.15	440	3.41
423	0.74	1,000	2.50	0.128	342	3.80
423	0.82	1,000	4.4	0.151	380	3.97
423	0.89	1,000	5.7	0.170	412	4.1
423	0.90	1,000	2.9	0.130	418	3.1
423	0.95	1,000	4.1	0.172	470	3.66
423	0.92	1,000	2.9	0.152	432	3.52
423	0.86	1,500	2.9	0.146	*	3.38
424	1.67	1,000	2.9	0.160	515	3.11
430	1.76	1,000	6.3	0.235	625	3.76
431	1.77	1,000	6.4	0.210	635	3.31
433	1.72	1,000	5.7	0.230	625	3.68

*For this run the correlation predicted a value of 516 m^{-1} for the interfacial area, although the experimental data of Sridhar et al. (1980b) indicate the effect of stirrer speed on the interfacial area to be negligible, so that the actual value may be much closer to the value at 1,000 rpm, 432 m.

agreed well. The values of the volumetric mass transfer coefficient reported in Table 3 have been calculated from the slope.

In Figure 9, the straight line for 423 K contains data points from two runs conducted at stirrer speeds of 1,000 and 1,500 rpm, but otherwise similar conditions. The values of the volumetric mass transfer coefficient, evaluated separately, are 0.152 for the 1,000 rpm run and 0.146 for the 1,500 rpm run, showing no effect of the stirrer speed in this range. This result is less surprising than it may seem, since the data of Sridhar et al. show the stirrer speed to have little effect on the interfacial area between 1,250 and 1,450 rpm at 423 K, and the present data as

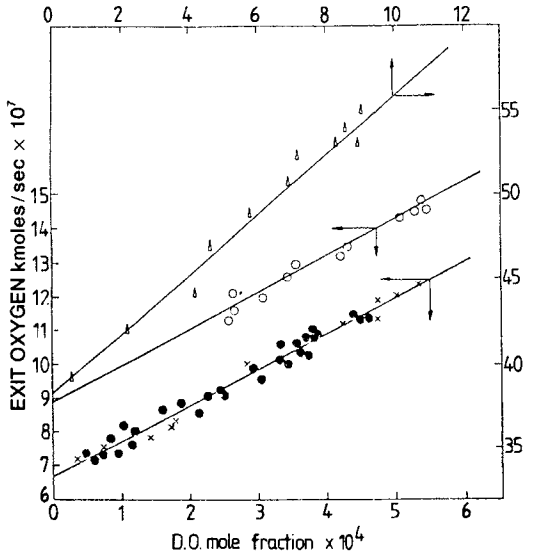

Figure 9. Relationship of EO-DO concentrations at various temperatures, inlet O_2 concentrations, stirrer speeds, and superficial gas velocities.

O 414.5 K; 3.6% O_2; 1,000 rpm; 0.98 × 10^{-2} m/s
● 423 K; 2.9% O_2; 1,500 rpm; 0.86 × 10^{-2} m/s
X 423 K; 2.9% O_2; 1,000 rpm; 0.92 × 10^{-2} m/s
△ 430K; 6.3% O_2; 1,000 rpm; 1.76 × 10^{-2} m/s

well as those of other workers in the literature show the effect of power input on the mass transfer coefficient to be small.

Some experiments were conducted at a higher superficial velocity of about 1.7 × 10^{-2} m/s. The values of k_La obtained in these cases were higher, but the values of k_L fall in the same general range as the values obtained at lower superficial velocities, again showing no effect of power input on the mass transfer coefficient.

The value of the mass transfer coefficient from all the runs during reaction, in the temperature range 413–435 K, are seen to fall in a narrow range of 3–4 × 10^{-4} m/s. In Figure 10, the mass transfer coefficients over the entire temperature range covered in this work, determined by both the physical method and the DO-EO plot, are plotted as a function of the molecular diffusivity. The comparison between the values obtained by the two methods at 423 K is seen to be good.

Despite the scatter, the mass transfer coefficients in this entire temperature range are seen to lie in a band of 2 × 10^{-4} m/s, which incidentally is the region in which the mass transfer coefficients for most bubbling systems lie, Table 4. However, what is remarkable about the data is that this relative constancy of mass transfer coefficients obtains despite a variation in the molecular diffusivity of about an order of magnitude. This offers problems for standard theories of mass transfer. The Calderbank and Moo-Young (1961) correlations are plotted for comparison in Figure 10, where a reasonable agreement is seen at the lower temperatures with the small-bubble correlation. However, the correlation performs increasingly poorly at higher temperatures, the values at 423–433 being overpredicted by a factor of three or more.

Since the diffusivity variation in the present case has been brought about by a change in temperature, the effect of the variation in other physical properties such as density, viscosity, and surface tension, and the possibility for such effects to counteract the influence of an increasing diffusivity should be considered. However, turning once again to the Calderbank and Moo-Young correlations to provide a basis for estimating such effects, we find that over the range of temperatures investigated, the variation in physical properties other than diffusivity is expected to have comparatively little effect on the mass transfer coefficient. In any case, the variation in these properties is only expected to enhance the effect of diffusivity on mass transfer coefficients.

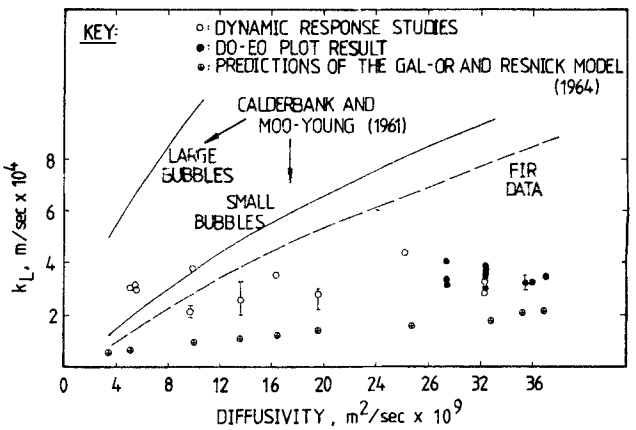

Figure 10. Observed variation of mass transfer coefficients with diffusivity.

Table 4. Mass Transfer Coefficients in Bubbling Systems

Gas-Liquid System	Contacting Conditions	Mass Trans. Coeff. $m/s \times 10^4$	Ref.
O_2-water	Spiral flow aeration tank (ambient)	2.5–4	Unno et al. (1983)
O_2-aqueous Na_2SO_3	Bubble columns and agitated vessels, sparged (ambient)	4	Reith & Beek (1968)
CO_2-water	Bubbles in free rise (ambient)	3–4	Bowman & Johnston (1962)
CO_2-water	Bubbles in free rise (ambient)	2–4	Calderbank & Lochiel (1964)
CO_2-water	Agitated vessel, sparged (ambient)	3–6	Prasher & Wills (1973)
O_2-water 10% CO_2-water 0% Cl_2-water He, H_2, O_2, CO_2, CH_4, C_2H_6, C_2H_2, C_2H_4 } water	Bubbles in free rise (ambient)	3–5 2.9–4	Li et al. (1968) Weller (1972)
H_2-edible oil	Agitated vessel, surface aerated (343 K)	1.5–2	Ganguli and ven den Berg (1980)
CO_2 { Xylene, Benzyl alcohol, Diethylene glycol, Cyclohexanol	Agitated vessel, sparged (ambient)	2–6	Sridharan & Sharma (1976)
CO-cuprous diethanol amine complex	Agitated vessel, sparged (ambient)	3–4	Sridharan & Sharma (1976)
CO-cuprous ammonium complex	Agitated vessel, sparged (ambient)	2–3	Sridharan & Sharma (1976)

A comparison between the mass transfer coefficients in the FIR with those in the STR reveals a few interesting features. First, at temperatures of 423–433 K the mass transfer coefficients in the FIR are about two to three times as large as those in the STR. This, in itself, is a fairly surprising result when one considers the vastly higher power input levels in the STR. In addition, when the FIR data are plotted (dashed line in Figure 10) as a function of diffusivity as before, the behavior is strikingly different from what was observed with the data from the STR. In this comparison, data at a constant stirrer speed of 150 rpm are shown. It is seen that the variation is qualitatively similar to the predictions of the Calderbank and Moo-Young correlations. This therefore suggests a fundamental difference in the mechanics of mass transfer between the free interface in the FIR and the bubble-liquid interface in the STR.

Thornton et al. (1985), using tracer visualization studies, have clearly established that surface renewal of drops does not take place. However Davies and Khan (1965) show that in flat interface reactors surface renewal can be demonstrated, using talc. These two studies then clearly establish that mass transfer across spherical surfaces and plane interfaces could be by different mechanisms. Using the plane interface reactors as a convenient model has been a common practice, but such use may not be warranted where application is made to an industrial reactor.

Extension of bubble-based theories to mass transfer from a bubble swarm has to take into account the possibility of interaction between bubbles. When bubbles are in close proximity, the concentration and velocity fields around one bubble can be influenced by those of its immediate neighbours and transfer rates can be reduced as a result. The gas holdup can thus be expected to enter into the governing equations, being a measure of the average distance between bubbles in a dispersion.

In comparing the present data with the correlations of Calderbank and Moo-Young, one must not lose sight of the fact that at the higher end of the temperature scale in the present studies, the viscosity and surface tension of the liquid are much lower than for the systems studied in their work. It is known that both the ratio of the viscosities of the dispersed to the continuous phase as well as the surface tension of the liquid have a profound effect on the internal circulation in the bubbles, and hence, one would expect, on the surface renewal rates. The viscosity ratio is usually negligible for gas-liquid systems. In the present case, the viscosity of a nitrogen-cyclohexane vapor mixture can be determined by the procedures outlined by Reid et al. (1977), and its ratio to the viscosity of liquid cyclohexane increases by a factor of 5 from ambient conditions to 423 K and 12 bar, but is still quite small (about 0.07) at 423 K. The surface tension of the liquid decreases by a factor of 2.5 for the same change in conditions.

The lowering of the surface tension, in particular, can bring about a market decrease in surface renewal rates that would oppose any increase in the mass transfer coefficient due to the increase in diffusivity. Further, the higher diffusivities, combined with the lower surface renewal rates, result in greater depths of penetration of the solute into the liquid film surrounding the bubbles and this would increase the chances of interaction between bubbles in a swarm. This can bring about a further

decrease in apparent mass transfer rates. The cumulative effect of such factors can, in principle, completely nullify any effect an increase in diffusivity might otherwise have had.

Experimental confirmation of these effects would presumably involve a determination of the mass transfer coefficients in other systems with similar diffusivities but different surface tension. No such systems under ambient conditions come to mind, and accurate determination of mass transfer coefficients at conditions of high temperature and pressure in a general system poses problems. However, an extreme case that has been theoretically investigated can be examined. This is the model of Gal-Or and Resnick (1964), which considers surface renewal to be practically absent during the life of a bubble.

Choosing the cell model (Happel, 1958) as a basis, Gal-Or and Resnick considered mass transfer to occur from a bubble to the liquid immediately in contact with it, the amount of liquid available for each bubble being determined by the gas holdup. The physical picture is thus not unlike that assumed in Ruckenstein's (1964) analysis described earlier, but an unsteady state transfer process is considered in this case and velocity gradients in the region of concentration variation are neglected. Mass transfer occurs for a time equal to the residence time of the bubble, at the end of which time the bubble escapes and the liquid gets mixed into the bulk. The expression of Gal-Or and Resnick for mass transfer can be written in terms of the concentration driving force at the inlet to the reactor

$$\frac{R_A}{a} = k_{LG}(c^* - c_1) \tag{11}$$

where the apparent mass transfer coefficient k_{LG}, defined by

$$k_{LG} = \frac{2r_b}{\pi^2\tau_G}(\phi - 1)\left\{\frac{\pi^2\tau_G D\phi}{2r_b^2(\phi-1)^2} - \sum_1^\infty \frac{1}{n^2}\exp\left[-\frac{n^2\pi D\tau_G}{r_b^2(\phi-1)^2} + \frac{\pi^2}{6}\right]\right\} \tag{12}$$

does not contain any fitted parameters. Although Gal-Or and Resnick eliminate the liquid concentration in Eq. 11 by assuming a pseudosteady state, it is perhaps preferable to leave the equations in the general form as above so that they are applicable to both steady and unsteady state situations. The correspondence between this and the penetration model becomes apparent when one notes that the notion of a contact time in the penetration theory has been replaced in the present model by the mean gas residence time.

Since the equations used in the evaluation of the mass transfer coefficients in the STR by the physical method essentially assume a driving force that corresponds to the inlet conditions, a comparison can be made between the present mass transfer coefficients and the values k_{LG} calculated from Eq. 12. Such calculations, for the conditions of the present experiments, gave values of k_{LG} that are practically identical at a given temperature. These values have therefore been shown by points on Figure 10, and show that while they are much lower than the experimental values at lower temperatures, they do approach the latter to within 50% at 423 K. This provides some evidence for the small surface renewal rates at high temperatures in the present system.

In order to look at the possibility of interaction between bubbles in at least an approximate sense, we examine the extent of the concentration profiles that develop around a spherical bubble which is transferring solute by unsteady state diffusion to the surrounding liquid. The relevant differential equation and the boundary conditions are

$$\frac{D}{r^2}\frac{\partial}{\partial r}\left(r^2\frac{\partial c}{\partial t}\right) = \frac{\partial c}{\partial t} \tag{13}$$

with

$$t = 0, c = c_1 \quad \text{in } r_b \leqq r \leqq b \tag{14}$$

$$t \geqq 0, c = c^* \quad \text{at } r = r_b \tag{15}$$

$$t \geqq 0, c = c_1 \quad \text{at } r = \infty \tag{16}$$

This equation is solved (Crank, 1964), and the solution is

$$\frac{c - c_1}{c^* - c_1} = \frac{r_b}{r}\,\text{erfc}\left[\frac{r - r_b}{2(Dt)^{1/2}}\right] \tag{17}$$

At a given value of the gas holdup H_G, the average distance between bubbles is given by

$$\phi = \frac{b}{r_b} = (H_G)^{-1/3} \tag{18}$$

where b is the outer radius of the spherical shell of liquid that surrounds each bubble, in the manner assumed by Gal-Or and Resnick.

If the time available for mass transfer is equal to the residence time of the bubble as assumed in the model of Gal-Or and Resnick, defining a depth of penetration from the value of r when the dimensionless concentration on the lefthand side of Eq. 17 gets down to a value of 0.01, we can calculate a value of the gas

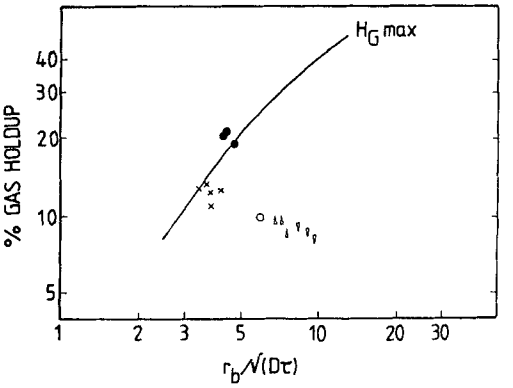

Figure 11. Gas holdup at which interaction between bubbles becomes significant in a swarm at various temperatures and gas velocities.

O 423–433 K, 1.7×10^{-2} m/s
● 393 K, 0.78×10^{-2} m/s
△ 353 K, 0.78×10^{-2} m/s
△ 353 K, 0.78×10^{-2} m/s
X 413–423K, 1×10^{-2} m/s
△ 373 K, 0.78×10^{-2} m/s

holdup beyond which the bubbles are, on an average, closer than this depth. This then would be the maximum gas holdup at which bubbles can exist without interaction in the swarm. In Figure 11, this holdup, H_{Gmax}, is plotted as a function of the parameter $r_b/(D\tau)^{1/2}$. Holdups estimated (using the correlation of Sridhar and Potter, 1980a) for a number of experiments in the present work are also shown on the same plot. An increasing possibility for interaction effects to modify observed mass transfer coefficients is seen at the higher temperatures. When the experimental holdup is as close to the H_{Gmax} curve as the data for temperatures of 413 to 435 K are in Figure 11, interaction must be considered a definite possibility, since the above analysis is only approximate and the estimation of gas holdup can involve considerable error. Further, the local variations in gas holdup, bubble radius, and even mass transfer coefficients in the STR might result in the effects of interaction being greatest in regions of the highest mass transfer coefficients (the impeller zone), and therefore the effects of interaction on the measured (global) transfer coefficient could be greater than the simple analysis above would indicate.

Conclusions

The solubility of oxygen in cyclohexane obeys Henry's law, and the Henry's law coefficient can be regarded as a constant at 1.09×10^{-2} kmol/m^{3}bar over the temperature range 293–435 K. The physical mass transfer coefficient in the bubble STR also shows very little variation over this temperature range. A value of 3.5×10^{-4} m/s can be assumed for this quantity at reaction temperatures of 423–435 K. The present data indicate that the popular correlations of mass transfer which have been found to hold under ambient conditions might lead to grossly erroneous predictions if they are extrapolated to the conditions of organic oxidations.

The data on the mass transfer coefficients in the FIR and the STR indicate a fundamental difference in the mass transfer behavior. While mass transfer coefficients in the FIR can be regarded as following the predictions of the popular theories of mass transfer by and large, their behavior in the STR shows anomalies, in that the mass transfer coefficients do not show the increases expected from the large increase in diffusivity that occurs over the temperature range. A reduction in the surface renewal rates, brought about as a result of the lowering of surface tension at high temperatures, together with a higher possibility of interaction between bubbles at the higher diffusivities, is suggested as the reason for this behavior. Although some support for such a mechanism is provided from the theoretical model of Gal-Or and Resnick (1964) and from a consideration of the penetration depths in unsteady state absorption from a sphere, more experimental data in other systems under similar conditions are necessary before the interplay of the various physical properties in determining the mass transfer rates in bubbling systems is fully understood.

Acknowledgment

S. Asai of Osaka Prefectural University helped with the reactor design for this project during a sabbatical leave at Monash University in 1973. The Australian Research Grants Scheme and Monash University Special Research Fund have provided support for this project, together with assistance from G. C. Jagirdar, S. Konstantinidis, and B. Butler.

Notation

a = interfacial area per unit volume of dispersion, m^2/m^3
a = interfacial area per unit volume of liquid, m^2/m^3
A = dimensionless group, $k_L a \tau_G$
b = outer radius of cell model, m
B = dimensionless group = $\beta V_L/N_G$
c_1 = concentration of dissolved gas in bulk liquid, kmol/m^3
c_{10} = oxygen concentration in initial steady state in step change experiments, kmol/m^3
c_1 = concentration
c_0 = concentration of dissolved gas (or oxygen) at any distance from interface, kmol/m^3
c^* = concentration of dissolved gas (or oxygen) at interface (equilibrium value), kmol/m^3
D = molecular diffusivity of gaseous solute in liquid phase (in particular, of oxygen in cyclohexane), m^2/s
d_T = tank diameter
G_1 = total molar flow rate of gases at inlet of contractor, kmol/s
G_2 = total molar flow rate of gases at outlet of contractor, kmol/s
H = Henry's law coefficient, mol frac/bar
H' = modified Henry's law coefficient, kmol/m^{3}bar, H_O oxygen, H_N nitrogen
H_{Gmax} = maximum value of gas holdup below which interaction between bubbles can be neglected
H_G = fractional gas holdup
H_L = fractional liquid holdup
I = intercept of dissolved oxygen-exit oxygen plot, kmol/s
k_L = physical mass transfer coefficient, m/s
$k_L a$ = volumetric mass transfer coefficient, physical, defined per unit dispersion volume, s^{-1}
K_{LG} = apparent overall liquid-side mass transfer coefficient, s^{-1}
N_G = number of moles of gas in contactor; in a bubbling contactor, number of moles of gas dispersed as bubbles
p' = exponent of diffusivity in theoretical expression for physical mass transfer coefficient
P = pressure
q_i = molar flow rate of oxygen into reactor, kmol/s
q_o = molar flow rate of oxygen out of reactor, kmol/s
r = radial distance from center of bubble, m
r_b = Sauter mean bubble radius, m
R_A = oxygen absorption rate per unit dispersion volume, kmol/m^{3}s
Sc = Schmidt number, $\mu/\rho D$
Sh_T = Sherwood number based on tank diameter, $k_L d_T/D$
t = time, s
$\bar{t}$ = dimensionless time $k_L at$
T = absolute temperature
U_G = superficial gas velocity, m/s
V_L = liquid volume, m^3
V_{GL} = dispersion volume, m^3
y_i = oxygen mole fraction in inlet gases, before step change
y_O = oxygen mole fraction in leaving gases, initial steady state
y_1 = oxygen mole fraction in inlet gases at $t \geq 0$
y_2 = oxygen mole fraction in leaving gases at any time
y = nondimensional form of oxygen mole fraction in gases

Greek letters

α = ratio of inlet molar flow rate to outlet molar flow rate
β = solubility of oxygen in cyclohexane, kmol/m^3
λ = roots of characteristic equation
μ = viscosity of liquid, kg/ms
ρ = liquid density, kg/m^3
ρ_m = molar density of liquid, kmol/m^3
τ_G = mean residence time of gas in contactor, s
ϕ = ratio of outer radius of cell model to bubble radius

Appendix

We consider a gas-liquid contactor that is batch with respect to the liquid and once-through with respect to the gas. In particular, we are interested in the transfer of oxygen from a stream of O_2-N_2-cyclohexane vapor into liquid cyclohexane. We assume the gas and liquid phases to be separately well mixed and allow

for the vaporization of some cyclohexane in the contactor, so that the inlet and exit flow rates of the gas are, even at small concentrations of the transferred solute, not equal in general. The molar flow rates at the inlet and outlet are related, however:

$$G_2 = \alpha G_1 \tag{A1}$$

α, which depends on the extent of evaporation in the contactor, can be determined from a knowledge of the condition of the entering gases (whether the nitrogen was presaturated with cyclohexane or not), the vapor pressure of cyclohexane at the operating temperature, and the operating pressure, assuming the gases to leave the contactor saturated with cyclohexane. Let the liquid be brought to a steady state with a gas flowing through the reactors. Let this initial steady state be characterized by an oxygen concentration of c_{10} in the liquid and an oxygen mole fraction y_o in the gases leaving the contactor. The two are related by the equilibrium relationship,

$$c_{10} = \beta y_o \tag{A2}$$

Further, with the liquid saturated with the gas in contact with it, no net transfer of solute takes place within the contactor and hence the composition of the inlet gas y_i is related to y_o by

$$y_i = \alpha y_o \tag{A3}$$

At time 0, let the composition of the inlet gas be changed instantaneously from y_i to y_1. We wish to follow the development of the new steady state. If y_2 is the exit mole fraction and c_1, the liquid concentration at any time t, N_G, the moles of gas in the contactor (in the case of the STR, N_G is the moles of gas dispersed in the liquid), and k_La, the volumetric mass transfer coefficient defined per unit volume of the liquid, we have for the oxygen in the gas phase

$$\frac{d(N_G y_2)}{dt} = G_1 y_1 - G_2 y_2 - k_L a V_L (c^* - c_1) \tag{A4}$$

and, for the liquid phase.

$$\frac{dc_1}{dt} = k_L a (c^* - c_1) \tag{A5}$$

with the initial conditions: $t = 0$, $y_2 = y_o$ and $c_1 = c_{10} = \beta y_o$.

Assuming equilibrium to prevail at the gas-liquid interface at all times,

$$c^* = \beta y_2 \tag{A6}$$

Using the following dimensionless variables,

$$\bar{y} = \frac{y_2 - y_0}{(y_1/\alpha) - y_0}; \bar{c} = \frac{c_1 - c_{10}}{(\beta y_1/\alpha) - c_{10}}$$

$$= \frac{c_1 - \beta y_0}{\beta[(y_1/\alpha) - y_0)]}; A = k_L a \tau_G$$

$$B = \beta V_L / N_G; \tau_G = N_G / G_2, \bar{t} = k_L a t$$

the equations and the initial conditions become,

$$\frac{d\bar{y}}{d\bar{t}} = \frac{(1 - \bar{y})}{A} - B(\bar{y} - \bar{c}_1) \tag{A7}$$

and

$$\frac{d\bar{c}_1}{d\bar{t}} = \bar{y} - \bar{c}_1 \tag{A8}$$

with

$$\bar{t} = 0, \bar{y} = 0, \text{ and } \bar{c}_1 = 0 \tag{A9}$$

The above equations can be reduced to a second-order differential equation and solved by the normal procedures (Keitel and Onken, 1981). The solution for the dissolved oxygen concentration can be written as

$$\bar{c}_1 = 1 + \frac{\lambda_2}{\lambda_1 - \lambda_2} \exp(\lambda_1 \bar{t}) - \frac{\lambda_1}{\lambda_1 - \lambda_2} \exp(\lambda_2 \bar{t}) \tag{A10}$$

where

$$\lambda_1 = -\frac{(1 + B + 1/A)}{2} + \frac{1}{2}[(1 + B + 1/A)^2 - 4/A]^{1/2} \tag{A11}$$

and

$$\lambda_2 = -\frac{(1 + B + 1/A)}{2} - \frac{1}{2}[(1 + B + 1/A)^2 - 4/A]^{1/2} \tag{A12}$$

Literature Cited

Astarita, G., *Mass Transfer with Chemical Reaction,* Elsevier, Amsterdam (1967).

Bowman, C. W., and A. I. Johnston, "Mass Transfer from Carbon Dioxide Bubbles Rising in Water," *Can. J. Chem. Eng.*, **40,** 139 (1962).

Calderbank, P. H., "Physical Rate Processes in Industrial Fermentation. II: Mass Transfer Coefficients in Gas-liquid Contacting with and without Mechanical Agitation," *Trans. Inst. Chem. Eng.*, **37,** 173 (1959).

———, "Gas Absorption from Bubbles," *Chem. Eng.*, CE209 (1967).

Calderbank, P. H., and A. C. Lochiel, "Mass Transfer Coefficients, Velocities and Shapes of Carbon Dioxide Bubbles in Free Rise through Distilled Water," *Chem. Eng. Sci.*, **19,** 485 (1964).

Calderbank, P. H., and M. B. Moo-Young, "The Continuous Phase Heat and Mass Transfer Properties of Dispersions," *Chem. Eng. Sci.*, **16,** 39 (1961).

Crank, J., "The Mathematics of Diffusion," 1st Ed., O.U.P., London (1964).

Cutter, L. A., "Flow and Turbulence in a Stirred Tank," *AIChEJ.*, **12,** 35 (1966).

Danckwerts, P. V., *Gas-Liquid Reactions, McGraw-Hill,* New York (1970).

Dang, N. D. P., D. A. Karrer, and I. J. Dunn, "Oxygen Transfer Coefficients by Dynamic Model Moment Analysis," *Biotechnol. Bioeng.*, **19,** 853 (1977).

Davies, J. T., and W. Khan, "Surface Clearing by Eddies," *Chem. Eng. Sci.*, **20,** 713 (1965).

Dunn, I. J., and A. Einsele, "Oxygen Transfer Coefficients by the Dynamic Method," *J. Appl. Chem. Biotechnol.*, **25,** 707 (1975).
Gallant, R. W., "Physical Properties of Hydrocarbons. I: Cyclic Hydrocarbons," *Hydroc. Process.*, **49,** 137 (1970).
Gal-Or, B., and Resnick, W. "Mass Transfer from Gas Bubbles in an Agitated Vessel with and without Simultaneous Chemical Reaction," *Chem. Eng. Sci.*, **19,** 653 (1964).
Ganguli, K. L., and H. J. van den Berg, "Liquid-side MTC for a Hydrogen-Edible Oil System in an Agitated Reactor," *Chem. Eng. J.*, **19,** 11 (1980).
Happel, J., "Viscous Flow in Multiparticle Systems, Slow Motion in Fluids Relative to Beds of Spherical Particles," *AIChE J.*, **4,** 197 (1958).
Hayduk, W., and W. D. Buckley, "Temperature Coefficient of Gas Solubility for Regular Solutions," *Can. J. Chem. Eng.*, **49,** 667 (1971).
Hughmark, G. A., "Holdup and Mass Transfer in Bubble Columns," *Ind. Eng. Chem. Process Des. Dev.*, **6**(2), 218, (1967).
Keitel, G., and U. Onken, "Errors in Determination of Mass Transfer in Gas-Liquid Dispersions," *Chem. Eng. Sci.*, **36,** 1927 (1981).
Linek, V., P. Benes, and F. Hovonka, "The Role of Interphase Nitrogen Transport in Dynamic Measurement of the Overall Volumetric Mass Transfer Coefficient in Air-sparged Systems," *Biotechnol. Bioeng.*, **23,** 301 (1981).
Linek, V., P. Benes, and F. Flovorka, "Analysis of Differences in k_LA Values Determined by Steady State and Dynamic Methods in Stirred Tanks," *Chem. Eng. J.*, **25,** 77 (1982).
Li, P. S., F. B. West, W. H. Vance, and R. W. Moulton, "Unsteady State Mass Transfer from Gas Bubbles—Liquid Phase Resistance," *AIChE J.*, **11**(4), 581 (1965).
Lynch, D. W., and O. E. Potter, "Determination of Nitrogen Diffusivities in Liquid Cyclohexane Over a Wide Temperature Range," *Chem. Eng. J.*, **15,** 197 (1978).
Mann, R., "Gas-Liquid Contacting in Mixing Vessels," *Inst. Chem. Eng. Indust. Fellowship Rept.*, Inst. Chem. Eng., Warwickshire, England (1983).
Midoux, N., and J. C. Charpentier, "Mechanically Agitated Gas-Liquid Reactors. 2: Interfacial Area," *Int. Chem. Eng.*, **24,** 452 (1984).
Prasher and G. B. Wills, "Mass Transfer in an Agitated Vessel," *Ind. Eng. Chem. Proc. Des. Dev.*, **12**(3), 351 (1973).
Reid, R. C., J. M. Prausnitz, and T. K. Sherwood, *The Properties of Gases and Liquids*, McGraw Hill, New York (1977).
Reith, T., and W. J. Beek, "Gas Holdups, Interfacial Areas, and Mass Transfer Coefficients in Gas-Liquid Contractors," *Proc. 4th Eur. Symp. Chem. React. Eng.*, Brussels, 191 (1968).
Resnick, W., and B. Gal-Or, "Gas-Liquid Dispersions," *Adv. Chem. Eng.*, **7,** 295 (1968).
Ruchti, G., I. J. Dunn, and J. R. Bourne, "Comparison of Oxygen Electrode Methods for the Measurement of k_LA," *Biotechnol. Bioeng.*, **23,** 277 (1981).
Ruchti, G., I. J. Dunn, and J. R. Bourne, "Practical Guidelines for the Determination of Oxygen Transfer Coefficients (K_La) with Sulfite Oxidation," *Chem. Eng. J.*, **30,** 29 (1985).
Ruckenstein, E., "On Mass Transfer in the Continuous Phase from Spherical Bubbles or Drops," *Chem. Eng. Sci.*, **19,** 131 (1964).
Rushton, J. H., E. W. Costich, and H. J. Everett, "Power Characteristics of Mixing Impellers," *Chem. Eng. Prog.*, **46,** 395 (1950).
Schaftlein, R. W., and T. W. F. Russell, "Two-phase Reactor Design, Tank-type Reactors," *Ind. Eng. Chem.*, **60**(5), 13 (1968).
Sharma, M. M., and P. V. Danckwerts, "Chemical Methods of Measuring Interfacial Area and Mass Transfer Coefficients in Two-fluid Systems," *Brit. Chem. Eng.*, **15**(4), 522 (1970).
Sherwood, T. K., R. L. Pigford, and C. R. Wilke, "Mass Transfer," McGraw-Hill, New York (1975).
Sideman, S., O. Hortacsu, and J. W. Fulton, "Mass Transfer in Gas-Liquid Contacting Systems," *Ind. Eng. Chem.*, **58**(7), 33 (1966).
Sridhar, T., "Mass Transfer in Cyclohexane Oxidation," Ph.D. Thesis, Dept. Chem. Eng., Monash Univ., Clayton, Australia (1978).
Sridhar, T., and O. E. Potter, "Predicting Diffusion Coefficients," *AIChEJ.*, **23,** 590 (1977).
———, "Interfacial Area Measurement in Gas-Liquid Agitated Vessels—Comparison of Techniques," *Chem. Eng. Sci.*, **33,** 1347 (1978).
———, "Gas Holdups and Bubble Diameters in Pressurized Gas-Liquid Stirred Vessels," *Ind. Eng. Chem. Fundam.*, **19,** 21 (1980a).
———, "Interfacial Areas in Gas-Liquid Stirred Vessels," *Chem. Eng. Sci.*, **35,** 683 (1980b).
Sridharan, K., and M. M. Sharma, "New Systems and Methods for the Measurement of Effective Interfacial Area and Mass Transfer Coefficients in Gas-Liquid Contactors," *Chem. Eng. Sci.*, **33,** 767 (1976).
Suresh, A. K. (Suresh A. Krishnamurthy), "Mass Transfer and Chemical Reaction in Cyclohexane Oxidation," Ph.D. Thesis, Dept. Chem. Eng., Monash Univ., Clayton, Australia (1986).
Thornton, J. D., T. J. Anderson, K. H. Javed, and S. K. Achwal, "Surface Phenomena and Mass Transfer Interactions in Liquid-Liquid Systems," *AIChEJ.*, **31,** 1069 (1985).
Unno, H., F. Kikuchi, and T. Akehata, "Oxygen Transfer in Spiral Flow Aeration Tank," *J. Chem. Eng. Japan*, **16**(6), 508 (1983).
van't Riet, K., "Review of Measuring Methods and Results in Nonviscous Gas-Liquid Mass Transfer in Stirred Vessels," *Ind. Eng. Chem. Process Des. Dev.*, **18**(3), 357 (1979).
Weller, K. R., "Mass Transfer from a Single Gas Bubble," *Can. J. Chem. Eng.*, **50,** 49 (1972).
Wild, J. W., T. Sridhar, and O. E. Potter, "Solubility of Nitrogen and Oxygen in Cyclohexane," *Chem. Eng. J.*, **15,** 209 (1978).
Yaws, C. L., and A. C. Turnbough, "Physical and Thermodynamic Properties–Cyclopropane, Cyclobutane, Cyclopentane, and Cyclohexane," *Chem. Eng.*, **82,** 119 (1975).

Manuscript received July 22, 1986, and revision received July 13, 1987.